Triplet-singlet conversion by broadband optical pumping

R. Horchani,[1] H. Lignier,[1] N. Bouloufa-Maafa,[1,2] A. Fioretti,[1] P. Pillet,[1] and D. Comparat[1]

[1]*Laboratoire Aimé Cotton, CNRS, Université Paris-Sud, Bâtiment 505, 91405 Orsay, France*
[2]*Université Cergy-Pontoise, 95000 Cergy-Pontoise, France*

We demonstrate the conversion of cold Cs_2 molecules initially distributed over several vibrational levels of the lowest triplet state $a^3 \Sigma_u^+$ into the singlet ground state $X^1 \Sigma_g^+$. This conversion is realized by a broadband laser exciting the molecules to a well-chosen state from which they may decay to the singlet state through two sequential single-photon emission steps: The first photon populates levels with mixed triplet-singlet character, making possible a second spontaneous emission down to several vibrational levels of the $X^1 \Sigma_g^+$ states. By adding an optical scheme for vibrational cooling, a substantial fraction of molecules are transferred to the ground vibrational level of the singlet state. The efficiency of the conversion process, with and without vibrational cooling, is discussed at the end of the article. The presented conversion is general in scope and could be extended to other molecules.

The last decade has witnessed increasing experimental efforts to produce large samples of ultracold molecules in a well-defined quantum state. Such samples constitute a very interesting basis for a great variety of studies ranging from controlled molecular dynamics [1] and anisotropic long-range interactions [2] to precision measurements [3] and quantum computing [4]. Internal-state manipulation of ultracold alkali-metal molecules has been in the spotlight with the stimulated Raman adiabatic passage (STIRAP) technique, which allows transfer, with near-unity efficiency, of weakly bound molecules produced by magnetoassociation in the lowest triplet state to the absolute singlet ground state [5,6]. However, this technique is not suited to samples of molecules distributed in several vibrational levels, such as those produced by the widespread technique of cold-atom photoassociation.

Motivated by the goal of finding general methods to achieve this transfer, we propose an optical scheme to move a whole vibrational distribution from a specific electronic state to another one of different multiplicity and parity. By combining this technique with our vibrational cooling technique [7], we are able to produce large samples of ultracold molecules in the lowest vibrational level of the ground state. This successful combination demonstrates the versatility of the optical vibrational cooling. Our demonstration relies on photoassociated ultracold Cs_2 molecules stabilized in a vibrational distribution of the lowest triplet state $a^3 \Sigma_u^+ (a)$ that a suitable laser converts into the ground singlet state $X^1 \Sigma_g^+$ (X). Such a scheme provides an alternative way to efficiently produce ground-state molecules with photoassociation that mostly works in forming molecules in the lowest triplet state [8]. In the case of our experiment, it forms twice the number of molecules in the absolute vibrational ground level than any other photoassociation (PA) scheme [9].

The triplet-singlet conversion is not straightforward because of the quantum selection rules imposed by electric dipole transitions. The multiplicity $2S + 1$, where S is the total spin quantum number, must be conserved, and moreover, in the case of homonuclear molecules, the *ungerade-gerade* parity must be changed ($u \leftrightarrow g$). The conversion of multiplicity can occur if an intermediate state of the transition process is a mixture of the initial and final multiplicities due to, for instance, a spin-orbit coupling. The choice of the transition steps, based on the study published in [10], is summarized in Fig. 1(b): Cs_2 molecules prepared in the a state are excited by a broadband laser to the $(2)^3 \Pi_g$ state from which they may decay in two steps: first to the intermediate mixed state $0_u^+ (A^1 \Sigma_u^+ + b^3 \Pi_u)$ and then to the X state. This decay channel is not unique, and molecules may dissociate or simply go back to the a state. It is important to note that the fraction of molecules going back to the a state can be re-excited as long as the broadband laser contains the suitable frequencies. In other words, the large laser bandwidth has two closely related roles: exciting several levels of the initial vibrational distribution and recycling decayed molecules in the a state.

Our experimental setup is based on a classical magneto-optical trap (MOT). It provides an atomic cloud of $\sim 10^7$ atoms at a temperature of ~ 150 μK with a peak density of $\sim 10^{11}$ atoms/cm^3. An experiment cycle lasts 100 ms. During the first 50 ms, three different lasers are simultaneously switched on and used for PA, internal conversion, and vibrational cooling. As molecules are not trapped, they fall freely under the influence of gravity and are available for manipulation and detection during a period of about 10 ms. We now describe these important steps in more detail.

The detection stage is realized by resonance enhanced two-photon ionization (RE2PI). To this end, we use a pulsed dye (DCM) laser pumped by the second harmonic of a pulsed Nd:YAG laser with a 7-ns pulse duration and 0.5-cm^{-1} linewidth (2 mJ per pulse). The two-stage ionization produces Cs_2^+ ions that are detected by three stacked microchannel plates. The spectroscopic signal is monitored on a fast oscilloscope performing an averaging over 10 cycles. By scanning the RE2PI wave number in the available range (15 800–16 100 cm^{-1}), we obtain an ionization spectrum whose lines reveal vibrational transitions either from the a state via the $(3)^3 \Sigma_g^+$ state [11] or the X state via the $C^1 \Pi_u$ or $D^1 \Sigma_u^+$ state [Fig. 1(c)] [12].

The photoassociation is achieved by focusing a 50-ms, 750-mW Ti:sapphire laser onto the MOT. When the PA wavelength is tuned into resonance, pairs of colliding atoms absorb
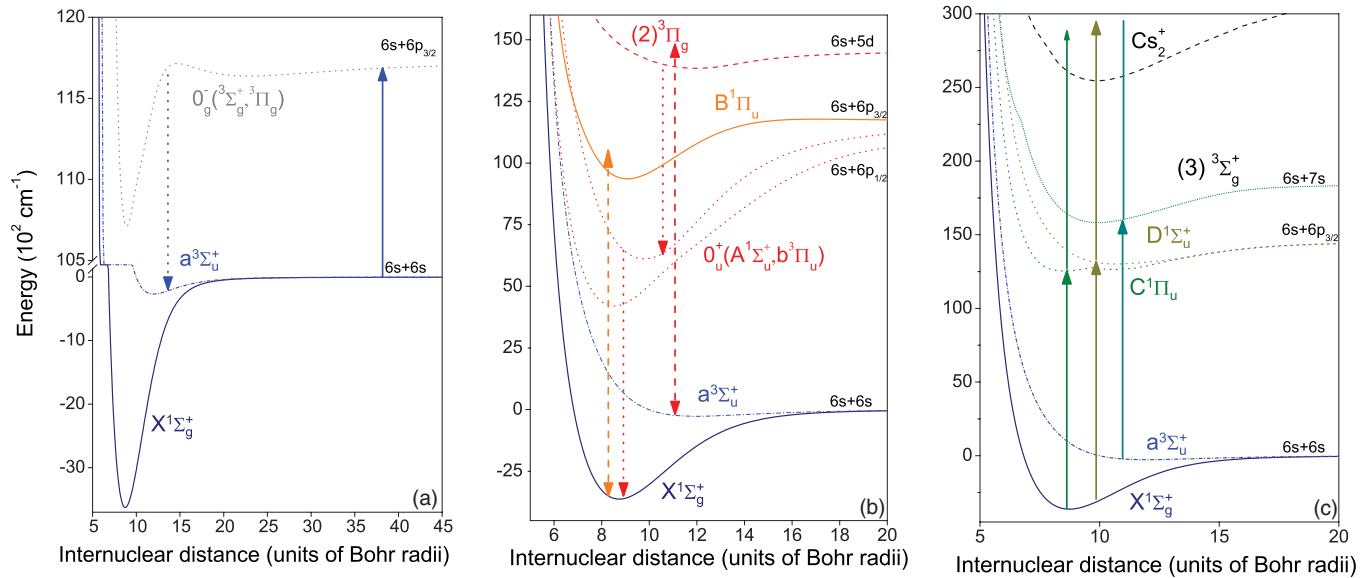
FIG. 1. (Color online) Transitions used to (a) photoassociate, (b) convert, cool, and (c) detect Cs_2 molecules. (a) Photoassociation: The PA laser frequency (solid up arrow) produces molecules in the a state after spontaneous emission (dotted down arrow). (b) Conversion: The laser used for conversion (dashed double arrow) transfers molecules from the a state to the $^3\Pi_g(6s + 5d)$ state. Apart from possible dissociation, two decay paths (dotted down arrows) may occur via spontaneous emission: toward the a state or toward the X state by passing through the mixed 0_u^+ states (two photons are involved). (c) Detection: Either in the a state or in the bottom of the X states, two-photon ionization allows detection of the vibrational populations (solid up arrows). In the case of the X state, the probed spectral range has two distinct possible transitions: through either $C^1\Pi_u$ or $D^1\Sigma_u^+$.

a photon to form molecules in an excited state, which are then stabilized by spontaneous emission [Fig. 1(a)]. In the following we consider only PA schemes which mainly populate the a state. We mainly used an efficient PA scheme identified by Fioretti *et al.* [13], denoted G_1, at the PA wave number $\tilde{\nu} = 11730.0422$ cm^{-1}. How the vibrational levels of the a state are populated depends upon the Franck-Condon (FC) factors between its 54 vibrational levels [14] and the PA excited level. To know the experimental vibrational distribution resulting from a given PA scheme, we performed RE2PI spectroscopy.

The triplet-singlet conversion is performed by femtosecond laser pulses (500 mW, 120 fs) tuned to ~13 910 cm^{-1} in order to induce $[(2)^3\Pi_g, \nu_\Pi] \leftarrow (a, \nu_a)$ transitions. As mentioned above, thanks to a two-photon cascade, the excited molecules are likely to end in the X state [Fig. 1(b)], thus realizing the intended conversion. Here the spectral width (~200 cm^{-1}) is the only interesting feature: It is larger than the energy range of the vibrational distribution (~50 cm^{-1}), which implies that all the vibrational populations in the a state are likely to be excited. This laser does not affect the populations in the X state.

A vibrational cooling scheme is then employed to pump converted molecules into $\nu_X = 0$ [7]. For this purpose, we use a laser diode running below its lasing threshold characterized by a spectral width of about 200 cm^{-1}. This light, with a spectrum centered at 12 940 cm^{-1}, causes multiple transitions between the X state and the $B^1\Pi_u$ state [Fig. 1(b)]. Because the part of the spectrum inducing transitions from $\nu_X = 0$ is removed by an interferential filter, molecules are progressively pumped down to that level [15]. As expected intuitively, as the laser spectral width becomes broader, the vibrational levels are pumped more efficiently. According to numerical simulations, a 200 cm^{-1} linewidth enables one to transfer a population

roughly spread over the 10 first vibrational levels to $\nu_X = 0$ with an efficiency greater than 90%. Molecules lying in higher levels also undergo transitions, but they slowly spread throughout the vibrational levels of the X state. We checked that vibrational cooling does not disturb the formation and conversion of molecules in the a state, meaning that all these processes can work simultaneously.

In order to demonstrate molecular conversion and vibrational cooling, four relevant configurations are discussed: (a′) PA only, (a) PA and vibrational cooling, (b) PA and laser conversion, and (c) PA, conversion laser, and vibrational cooling. The corresponding RE2PI spectra have been systematically recorded and subjected to a fitting procedure considering the possible vibrational transitions shown in Fig. 1(c) and their characteristics [11,12], that is, the transition energies, the FC factors, the average electrical transition dipole moments (TDM), and also the linewidth of the pulsed dye laser. This gives us the vibrational populations of the a and X states for each configuration.

In the (a) configuration, we obtained the typical RE2PI spectrum shown in Fig. 2(a). Although the PA scheme essentially produces molecules in the a state, a fraction of those are stabilized in the X state through a two-photon decay process (equivalent to [7,16]). In order to quantify the number of molecules initially in the X state, we added the vibrational cooling to PA and obtained the spectrum shown in Fig. 2(b). Although the RE2PI spectra obtained with and without vibrational cooling look very similar, we note that a few peaks appear when vibrational cooling is used. The positions of these peaks exactly correspond to $(C, \nu_C) \leftarrow (X, \nu_X = 0)$ transitions, which confirms that the vibrational populations of the X state are pumped to $\nu_X = 0$. The rest of
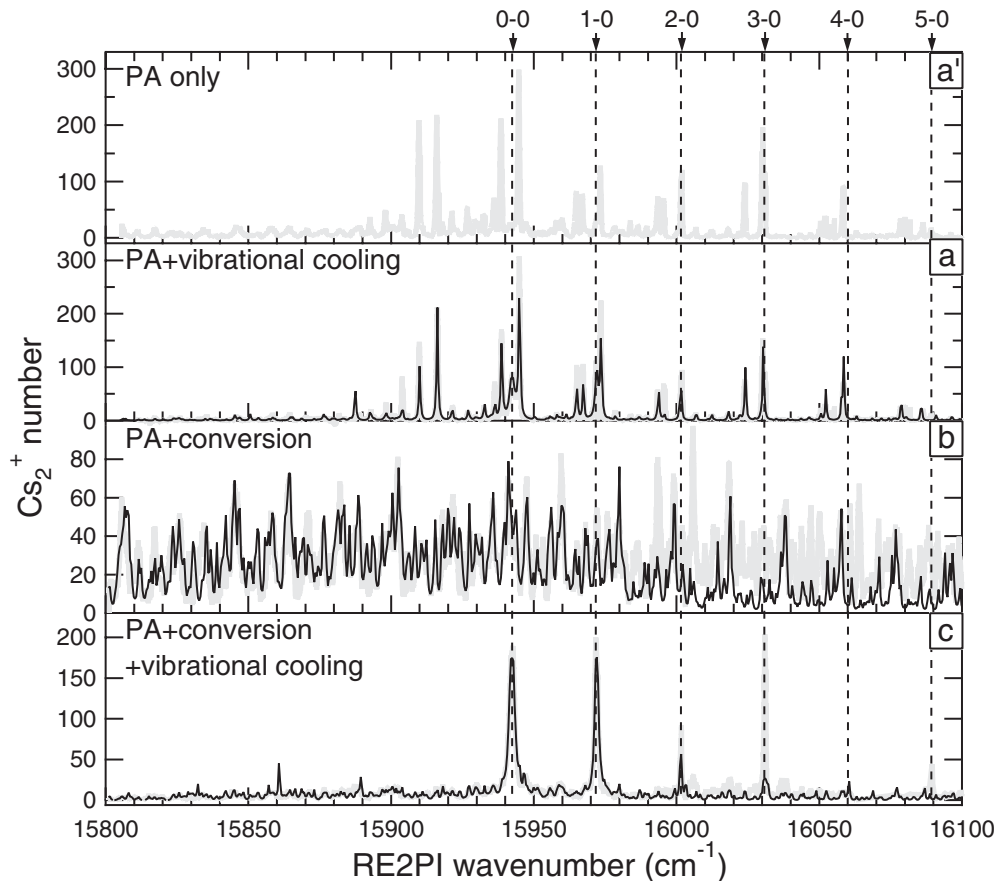
FIG. 2. RE2PI spectra (thick gray lines) and their fits (thin black lines) in four cases: (a′) PA spectrum revealing the lines from the $a^3 \Sigma_u^+$ state (fit not shown). (a) PA with vibrational cooling: Thus, the vibrational series of the X state has been reduced to a few lines corresponding to the $v_X = 0$ population. (b) When the conversion laser is added to PA only, the previous spectrum undergoes strong modifications. (c) The same as (b) with vibrational pumping: Intense peaks corresponding to $v_X = 0$ emerge whereas the lines from the $a^3 \Sigma_u^+$ state have apparently disappeared. Above the graph, the numbers associated to the arrows represent the vibrational numbers of the $(C, v_C) \leftarrow (X, v_X = 0)$ transitions.

the spectrum (i.e., the lines belonging to the vibrational series of the a state) is not affected by this manipulation. The interest of such a spectral "cleaning" is to improve the results of our fitting procedure and make molecules visible that will not be mistaken for those that will result from the conversion process. The fitting procedure indicates, with good reliability, that 90% of molecules decayed in the a state are gathered in the range $18 \lesssim v_a \lesssim 26$ [Fig. 3(a)], while the rest can be put into the $v_X = 0$ level [Fig 3(a)].

In the (b) configuration, the RE2PI spectrum is deeply modified as it is visible in the spectrum shown in Fig. 2(b). This spectrum shows a high line density, suggesting that the initial populations of the a state have been redistributed among numerous levels. A visual inspection of the spectrum ensures that a part of the molecules reaches the X state because many lines are found below 15 827 cm^{-1}, which is the cutoff wave number under which there is no transition from the a state. Due to the partial knowledge of the transition characteristics, our fitting procedure encounters limitations, especially for spectral regions above 16 000 cm^{-1}. Yet it shows that the X state is much more populated than previously as suggested by the comparison between the distributions (a) and (b) in Fig. 3(b).

The (c) configuration, where vibrational cooling is added to the conversion, definitively demonstrates that molecules

have been transferred to the X state. We effectively note that the RE2PI spectrum, displayed in Fig. 2(c), consists of intense peaks, proving an accumulation of molecules in $v_X = 0$, and a background of small lines arising from molecules that escape from either the vibrational pumping or the conversion scheme. The results of the fitting procedure shown in Fig. 3(c), compared to the situation of Fig. 3(a), confirm that the population in $v_X = 0$ has clearly increased while the distribution in the a state has decreased and changed.

With this, it is clear that molecules undergo a triplet-singlet conversion under the action of our scheme. The fitting procedure indicates that the increment of $v_X = 0$ population compared to the initial number of molecules in the a state reaches about 10% when the laser conversion and vibrational cooling process are applied. We can deduce that 10% is a lower limit to the efficiency of the sole conversion toward the X state since the vibrational cooling is not 100% efficient. Our fitting procedure might be considered as a good and general method to estimate this efficiency. However, when the spectrum is too dense, like that obtained with configuration (b), the vibrational distributions obtained are not reliable.

To improve our understanding and confirm our raw observations, we numerically simulated the conversion process
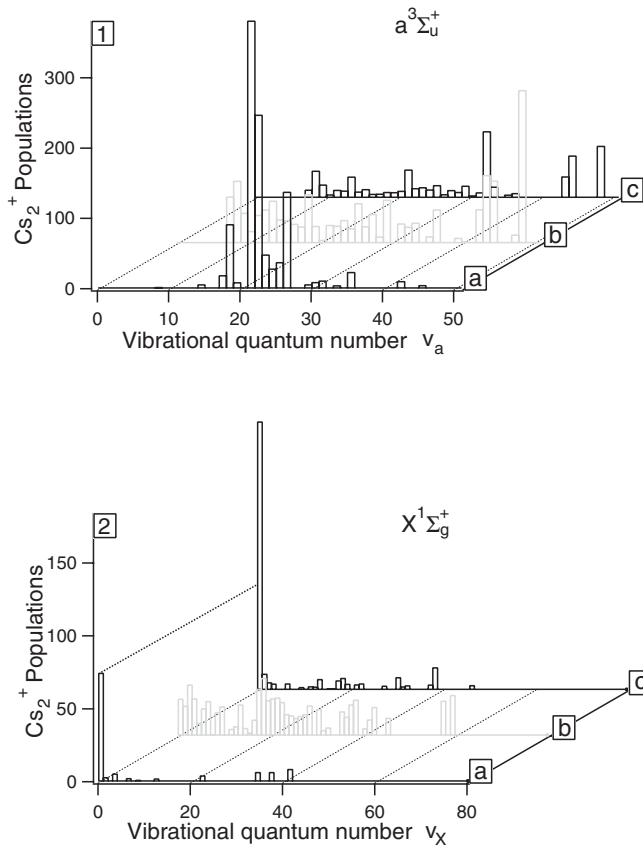
FIG. 3. Vibrational distributions of the *a* state (1) and the *X* state (2) obtained by fitting the spectra of Figs. 2(a), 2(b), and 2(c). The distributions (a) and (c) are well determined given that the line densities of their respective spectra are low enough to enable a reliable fit. Here the use of vibrational cooling shows that the population of $v_X = 0$ roughly doubles when the conversion laser is applied. The quality of the (b) distribution is questionable as the integrated number of molecules is distinctly too high.

and vibrational cooling. This simulation starts from the initial vibrational distribution of the *a* state, displayed in Fig. 3(a), and computes the evolution of the initial population submitted to the conversion laser. According to its wavelength and width, this laser enables to reach only the $0_g^\pm$ components; that is, the lowest fine structure components of the $(2)^3 \Pi_g$ state [17]. The spontaneous emission from the $0_g^\pm$ components can then populate the $0_u^+(A^1 \Sigma_u^+, b^3 \Pi_u)$, $0_u^-[(2)^3 \Sigma_u^+, b^3 \Pi_u]$, and $1_u[(2)^3 \Sigma_u^+, b^3 \Pi_u, B^1 \Pi_u]$, all of them being components of the $(b)^3 \Pi_u$ state. We consider that 0_u^- and 1_u states are both metastable: The only possible decay respectively occurs by quadrupolar transition (to the *a* state) and weak dipolar transition (to the *X* state) due to the $B^1 \Pi_u$ component. We assume that the lifetime of these states is so long that molecules reaching them are lost in the experiment. This assumption is supported by the fact that we do not see any long time dynamics in the conversion process. On the contrary, the 0_u^+ state can efficiently decay to the *X* state through its $A^1 \Sigma_u^+$ component. Consequently, our simulation considers the only path leading to the *X* state in times that make the experimental detection possible: $(2)^3 \Pi_g \longleftrightarrow a$, $(2)^3 \Pi_g \to 0_u^+(A^1 \Sigma_u^+, b^3 \Pi_u)$, $0_u^+(A^1 \Sigma_u^+, b^3 \Pi_u) \to X$. We
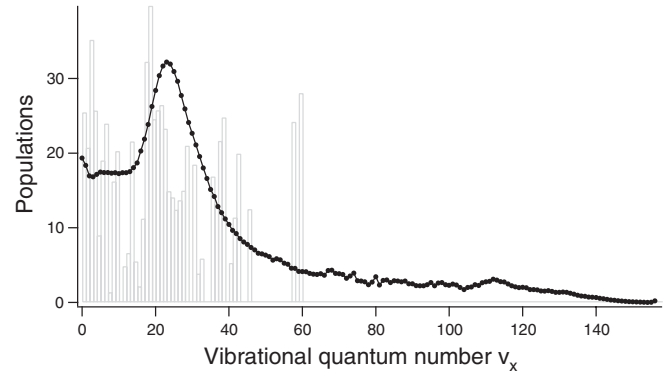

FIG. 4. Comparison of the vibrational distributions of the *X* state obtained by the numerical simulation (dots) and the fitting procedure [bars, same as Fig. 3(b)] when only the conversion process is applied. The absolute numbers of molecules per v_X are different but the general behaviors are similar: The low levels are mostly populated whereas there are few molecules above $v_X \approx 40$.

took into account the width of the conversion laser, the transition energies, the FC factors, and the average TDMs, ingredients that can be found in more detail in [10]. We note that molecules excited in the $(2)^3 \Pi_g$ state preferentially decay back to the *a* state because the TDM of this transition is about nine times larger than the TDM of the transition leading to $0_u^+(A^1 \Sigma_u^+, b^3 \Pi_u)$. This unfavorable feature does not really affect the whole conversion process because the width of the conversion laser enables molecular repumping from almost all the vibrational levels of the *a* state until they decay to 0_u^+. Only the last vibrational levels of the *a* state near the dissociation limit have extremely weak FC factors and are not recycled. Yet, as the distribution of the FC factors does not favor the accumulation of molecules in these high levels, only 3% of the molecules are lost in this way. Our simulation also takes into account the dissociation events that occur in small proportions (10%). The remaining molecules (87%) decay to the intermediate states, and a fraction of them eventually end up in the *X* state. In Fig. 4, the vibrational distribution in the *X* state obtained by the fitting procedure [Fig. 3(b)] and the numerical simulation are compared. Although the populations for a given v_X are different, both are spread over the same region of the *X* state (i.e., between $v_X = 0$ and $v_X \approx 40$). These differences between the populations are not surprising due to the limitations of the fitting procedure and the use of imperfect parameters in the numerical simulation. Finally, by adding the vibrational cooling to our simulation, we find that about 40% of the molecules reaching the *X* state are accumulated in $v_X = 0$. A marginal part is lost by dissociation and the rest by diffusion throughout the high vibrational levels of the *X* state. This implies that a higher value could be reached by using a broader linewidth laser for the vibrational cooling scheme. However, we find that the number of molecules reaching $v_X = 0$ is about three times greater in the simulation than in the experiment. This expected discrepancy supports the idea that some molecules are blocked in the metastable states and remain undetected.

We also experimentally tested the robustness of the cooling and conversion process with other initial vibrational distributions in the *a* state, by using other PA schemes. We used

transitions toward $[0_g^-(P_{3/2}), v=6, J=2]$ at $\tilde{v} = 11665.2055$ cm^{-1} [13] and $[0_g^-(P_{1/2}), v=32]$ at $\tilde{v} = 11158.5252$ cm^{-1} [16] that respectively form molecules in $37 \lesssim v_a \lesssim 50$ and in the highest levels of the a state. The latter distribution is not transferred by our conversion scheme, which is consistent with the previously evoked poor FC factors between the a state and $(2)^3\Pi_g$. On the other hand, the distribution with $37 \lesssim v_a \lesssim 50$ is converted in similar proportion to G_1.

In this work, we have been able to produce a large sample of molecules in the absolute vibrational ground state, albeit formed by PA in the lowest triplet state. The conversion process relies on the proposal described in Bouloufa *et al.* [10], except that, as suggested at the end of the same article, we make use of a broadband rather than a single-mode conversion laser. This modification explains why we detect 20 times more molecules in the X state and, if vibrational cooling is added, even

700 times more in $v_X = 0$ than predicted in [10]. On the other hand, it must be noted that the conversion process and vibrational cooling increase the rotational temperature. The reason is that each photon absorption or emission is likely to change the rotational quantum number by unity, and thus many transition processes provoke a population spread over of the rotational levels (i.e., a rotational heating).

[1] R. V. Krems, Phys. Chem. Chem. Phys. **10**, 4079 (2008).

[2] K.-K. Ni, S. Ospelkaus, D. J. Nesbitt, J. Ye, and D. S. Jin, Phys. Chem. Chem. Phys. **11**, 9626 (2009).

[3] O. Dulieu and C. Gabbanini, Rep. Prog. Phys. **72**, 086401 (2009).

[4] L. Carr, D. DeMille, R. Krems, and J. Ye, New J. Phys. **11**, 055049 (2009).

[5] F. Lang, K. Winkler, C. Strauss, R. Grimm, and J. Hecker-Denschlag, Phys. Rev. Lett. **101**, 133005 (2008).

[6] K. Ni, S. Ospelkaus, M. H. G. de Miranda, A. Pe'er, B. Neyenhuis, J. J. Zirbel, S. Kotochigova, P. S. Julienne, D. S. Jin, and J. Ye, Science **322**, 231 (2008).

[7] M. Viteau, A. Chotia, M. Allegrini, N. Bouloufa, O. Dulieu, D. Comparat, and P. Pillet, Science **321**, 232 (2008).

[8] K. M. Jones, E. Tiesinga, P. D. Lett, and P. S. Julienne, Rev. Mod. Phys. **78**, 483 (2006).

[9] M. Viteau, A. Chotia, M. Allegrini, N. Bouloufa, O. Dulieu, D. Comparat, and P. Pillet, Phys. Rev. A **79**, 021402 (2009).

[10] N. Bouloufa, M. Pichler, M. Aymar, and O. Dulieu, Phys. Rev. A **83**, 022503 (2011).

[11] N. Bouloufa, E. Favilla, M. Viteau, A. Chotia, A. Fioretti, C. Gabbanini, M. Allegrini, M. Aymar, D. Comparat, O. Dulieu *et al.*, Mol. Phys. **108**, 2355 (2010).

[12] C. Amiot, W. Demtröder, and C. R. Vidal, J. Chem. Phys. **88**, 5265 (1988).

[13] A. Fioretti, D. Comparat, C. Drag, C. Amiot, O. Dulieu, F. Masnou-Seeuws, and P. Pillet, Eur. Phys. J. D **5**, 389 (1999).

[14] F. Xie, V. B. Sovkov, A. M. Lyyra, S. I. D. Li, J. Bai, V. S. Ivanov, S. Magnier, and L. Li, J. Chem. Phys. **130**, 051102 (2009).

[15] D. Sofikitis, R. Horchani, X. Li, M. Pichler, M. Allegrini, A. Fioretti, D. Comparat, and P. Pillet, Phys. Rev. A **80**, 051401 (2009).

[16] H. Lignier, A. Fioretti, R. Horchani, C. Drag, N. Bouloufa, M. Allegrini, O. Dulieu, L. Pruvost, P. Pillet, and D. Comparat, Phys. Chem. Chem. Phys. **13**, 18910 (2011).

[17] H.-G. Krämer, M. Keil, J. Wang, R. Bernheim, and W. Demtröder, Chem. Phys. Lett. **272**, 391 (1997).